Measured Solid State and Sub-Cooled Liquid Vapour Pressures of Benzaldehydes Using Knudsen Effusion Mass Spectrometry

Petroc Shelley [1,*], Thomas J. Bannan [1], Stephen D. Worrall [2], M. Rami Alfarra [1,3], Carl J. Percival [4], Arthur Garforth [5] and David Topping [1]

1 Department of Earth and Environmental Sciences, The University of Manchester, Manchester M13 9PL, UK; Thomas.bannan@manchester.ac.uk (T.J.B.); rami.alfarra@manchester.ac.uk (M.R.A.); david.topping@manchester.ac.uk (D.T.)
2 Aston Institute of Materials Research, School of Engineering and Applied Science, Aston University, Birmingham B4 7ET, UK; s.worrall@aston.ac.uk
3 National Centre for Atmospheric Science (NCAS), The University of Manchester, Manchester M13 9PL, UK
4 NASA Jet Propulsion Laboratory, California Institute of Technology, 4800 Oak Grove Dr, Pasadena, CA 91109, USA; carl.j.percival@jpl.nasa.gov
5 Department of Chemical Engineering & Analytical Science, The University of Manchester, Manchester M1 3AL, UK; arthur.garforth@manchester.ac.uk
* Correspondence: petroc.shelley@manchester.ac.uk

Abstract: Benzaldehydes are components of atmospheric aerosol that are poorly represented in current vapour pressure predictive techniques. In this study the solid state (P_S^{sat}) and sub-cooled liquid saturation vapour pressures (P_L^{sat}) were measured over a range of temperatures (298–328 K) for a chemically diverse group of benzaldehydes. The selected benzaldehydes allowed for the effects of varied geometric isomers and functionalities on saturation vapour pressure (P^{sat}) to be probed. P_S^{sat} was measured using Knudsen effusion mass spectrometry (KEMS) and P_L^{sat} was obtained via a sub-cooled correction utilising experimental enthalpy of fusion and melting point values measured using differential scanning calorimetry (DSC). The strength of the hydrogen bond (H-bond) was the most important factor for determining P_L^{sat} when a H-bond was present and the polarisability of the compound was the most important factor when a H-bond was not present. Typically compounds capable of hydrogen bonding had P_L^{sat} 1 to 2 orders of magnitude lower than those that could not H-bond. The P_L^{sat} were compared to estimated values using three different predictive techniques (Nannoolal et al. vapour pressure method, Myrdal and Yalkowsky method, and SIMPOL). The Nannoolal et al. vapour pressure method and the Myrdal and Yalkowsky method require the use of a boiling point method to predict P^{sat}. For the compounds in this study the Nannoolal et al. boiling point method showed the best performance. All three predictive techniques showed less than an order of magnitude error in P_L^{sat} on average, however more significant errors were within these methods. Such errors will have important implications for studies trying to ascertain the role of these compounds on aerosol growth and human health impacts. SIMPOL predicted P_L^{sat} the closest to the experimentally determined values.

Keywords: secondary organic aerosol; vapour pressure; KEMS; group contribution method (GCM); benzaldehyde

1. Introduction

Climate and air quality are both significantly influenced by atmospheric aerosols, of which organic aerosols (OA) are a major component [1]. The composition of atmospheric aerosols can vary significantly by region, with OA contributing ~20 to 50% of total aerosol mass at continental mid latitudes, but being as high as 90% in some tropical forested areas [2]. Understanding the behaviours and properties of OA is essential to accurately predict their impacts on climate and human health. Currently, there are substantial uncertainties surrounding many of the physicochemical properties of atmospheric aerosols [3].

OA consist of primary organic aerosols (POA), which are emitted directly into the atmosphere as particulates, and secondary organic aerosols (SOA), which typically form when gas phase organic compounds in the atmosphere undergo oxidation. The products of these oxidation reactions tend to have lower vapour pressures then the reactants and are more likely to partition to the aerosol phase [2]. To predict whether a compound will partition, knowledge of its pure component equilibrium vapour pressure, also known as saturation vapour pressure (P^{sat}), is required [4]. Due to the complexity of the organic fraction of atmospheric aerosols, estimated to contain over 100,000 distinct organic species [5], and a lack of experimental data, the P^{sat} of many compounds must be estimated.

The most common way of estimating P^{sat} is using group contribution methods (GCMs). GCMs are based on the principle that functional groups within a molecule contribute additively to the property of interest. However, as compounds become more functionalised, the interaction between functional groups within a compound means this is often not the case. The Nannoolal et al. method [6], the Myrdal and Yalkowsky method [7], SIMPOL [8] and EVAPORATION (Estimation of VApour Pressure of Organics, Accounting for Temperature, Intramolecular, and Non-additivity effects) [9] are among the most common GCMs that are used for predicting P^{sat}. Both Barley and McFiggans (2010) [10] and O'Meara et al. (2014) [11] performed detailed assessments for these techniques comparing predicted and experimental P^{sat} for a range of compounds selected for their particular relevance to the formation of atmospheric aerosols. In both studies there was significant disagreement between the experimental and predicted P^{sat} for many of the compounds involved. Several of the older GCMs were developed primarily for use with higher volatility hydrocarbons or monofunctional compounds, whereas SOA are lower volatility and often highly functionalised. EVAPORATION [9] was developed specifically for predicting the P^{sat} of OA and the assessment by O'Meara et al. (2014) [11] showed the best performance for the compounds to which it was applicable. This highlights two larger issues GCMs have when predicting the P^{sat} of SOA. The older and more widely applicable methods show larger errors as P^{sat} decreases, while the newer and more targeted methods are limited by the functionalities represented within the data set they are fit to. Further development of new GCMs to expand the range of compounds to which they are applicable is limited by a lack of experimental data for the P^{sat} of relatively low volatility multifunctional compounds. GCMs also struggle to account for the impacts the relative positions of the functional groups can have on the P^{sat}, as well as the effects of internal interactions between functional groups on a compound of interest.

This work builds on previous work by Booth et al. (2012) [12], Dang et al. (2019) [13] and Shelley et al. (2020) [14] investigating the impacts of functional group positioning and the interaction of functional groups within a molecule on P^{sat}. In previous work by Shelley at al. (2020) [14] large absolute differences between experimental and estimated P^{sat} were observed, especially for nitrophenol compounds. One of the major reasons for these differences was due to the lack of previous experimental P^{sat} data for compounds with similar functionalities. Similar to nitroaromatics, benzaldehydes also have a lack of experimental P^{sat} data available. In this study the solid state saturation vapour pressure (P^{sat}_S) of atmospherically relevant benzaldehydes and other benzaldehydes of similar functionalities are determined using Knudsen Effusion Mass Spectrometry (KEMS). A sub-cooled correction is then made using data obtained using differential scanning calorimetry (DSC) to calculate the sub-cooled liquid saturation vapour pressures (P^{sat}_L).

Benzaldehydes have both anthropogenic [15] and biogenic sources [16] and can be emitted directly into the atmosphere or formed as secondary pollutants [17]. The major primary source for benzaldehydes is the direct emission from vehicle exhausts and they are therefore ubiquitous in the polluted urban atmosphere, with undiluted emissions from engines containing up to several hundred ppb [18]. Engine emission studies have found benzaldehydes from both diesel and biodiesel powered engines [19], as well as from petrol and petrol/ethanol blended powered engines [20]. Benzaldehydes are also produced in situ within the atmosphere and act as intermediates in the oxidation of aromatic compounds [15].

Benzaldehydes have also been observed in multiple atmospheric chamber experiments such as those by Hamilton et al. (2005) investigating the photo-oxidation of toluene in a large volume smog chamber [21] and those by Caralp et al. (1999) investigating the reaction kinetics of benzoyl and peroxybenzoyl radicals in a smog chamber [15]. Benzaldehydes are present in the Master Chemical Mechanism (MCM v3.2) [22,23] as precursors, reactants and products. Benzaldehydes are therefore an important class of compounds to have accurate measurements of P_L^{sat}, which are then compared to the predicted P_L^{sat} values of multiple GCMs to highlight areas of uncertainty. This will enable studies trying to ascertain the role of benzaldehydes on aerosol growth and human health impacts to be supported by accurate experimental data.

In this work P_S^{sat} and P_L^{sat} values are presented for 17 benzaldehydes. The P_S^{sat} values are compared to each other and chemical and steric arguments are given to explain the observed trends and differences. Following on from this, the experimental P_L^{sat} values and predicted P_L^{sat} values from several GCMs are compared. In this comparison areas and functionalities that perform well, as well as those that perform poorly are highlighted and recommendations for the GCM most suited to predicting benzaldehydes are made.

2. Experimental

A total of 17 benzaldehydes were selected for this study, shown in Table 1. All compounds selected for this study were purchased at a purity of 99% and used without further preparation. All compounds are solid at room temperature. The compounds selected cover a range of functionalities in addition to benzaldehyde including phenol, amino, ether, ester, and carboxylic acid. Several compounds also contain more bulky ethyl groups that can disrupt intermolecular interactions. Of the 17 compounds selected 8 can form H-bonds.

Table 1. Benzaldehydes measured with the Knudsen effusion mass spectrometry (KEMS). Compounds above the dashed line are capable of H-Bonding in the pure component and those below cannot.
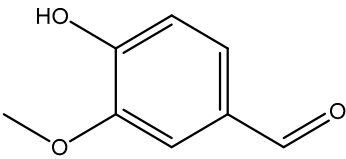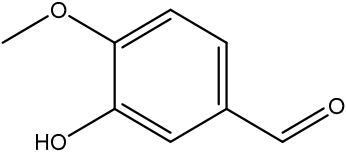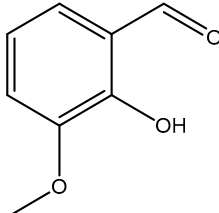
Compound	Structure	CAS	Supplier
Vanillin (4-hydroxy-3-methoxybenzaldehyde)		121-33-5	Sigma Aldrich
Isovanillin (3-hydroxy-4-methoxybenzaldehyde)		621-59-0	Sigma Aldrich
o-vanillin (2-hydroxy-3-methoxybenzaldehyde)		148-53-8	Fisher Scientific

Table 1. *Cont*.
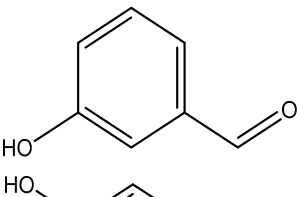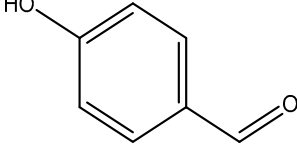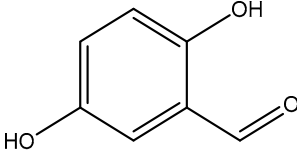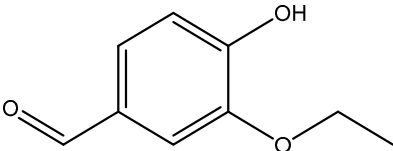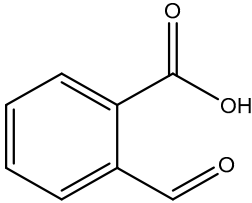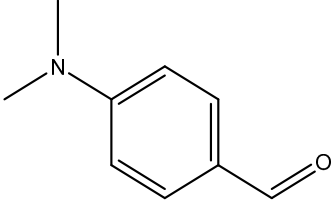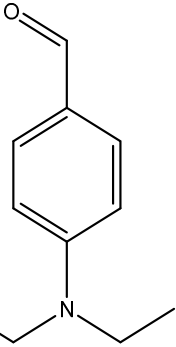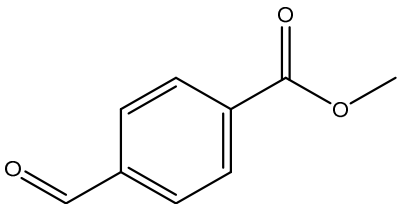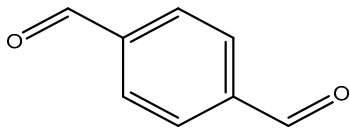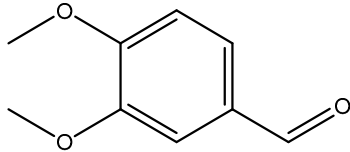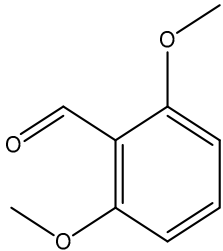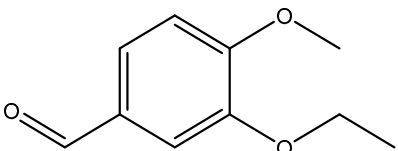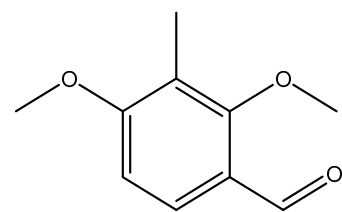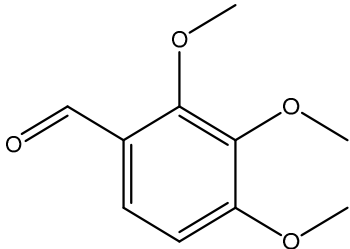
Compound	Structure	CAS	Supplier
3-hydroxybenzaldehyde		100-83-4	Sigma Aldrich
4-hydroxybenzaldehyde		123-08-0	Fisher Scientific
2,5-dihydroxybenzaldehyde		1194-98-5	Fisher Scientific
3-ethoxy-4-hydroxybenzaldehyde		121-32-4	Sigma Aldrich
2-formylbenzoic acid		119-67-5	Fisher Scientific
4-dimethylaminobenzaldehyde		100-10-7	Fisher Scientific
4-diethylaminobenzaldehyde		120-21-8	Sigma Aldrich

Table 1. *Cont*.

Compound	Structure	CAS	Supplier
methyl-4-formylbenzoate		1571-08-0	Sigma Aldrich
terephthalaldehyde		623-27-8	Sigma Aldrich
3,4-dimethoxybenzaldehyde		120-14-9	Sigma Aldrich
2,6-dimethoxybenzaldehyde		3392-97-0	Alfa Aesar
3-ethoxy-4-methoxybenzaldehyde		1131-52-8	Sigma Aldrich
2,4-dimethoxy-3-methylbenzaldehyde		7149-92-0	Sigma Aldrich
2,3,4-trimethoxybenzaldehyde		2103-57-3	Sigma Aldrich

2.1. The Knudsen Effusion Mass Spectrometry System (KEMS)

KEMS is an established vapour pressure measurement technique capable of measuring vapour pressures from 10^1 to 10^{-8} Pa. The KEMS system is the same instrument that has been used in previous studies [4,14,24,25] and a summary of the measurement procedure will be given here. For a more detailed overview see Booth et al. (2009) [25]. To calibrate the KEMS, a reference compound of known P^{sat} is used. In this study the polyethylene

glycol series (PEG series), PEG-3 ($P_{298} = 6.68 \times 10^{-2}$ Pa) and PEG-4 ($P_{298} = 1.69 \times 10^{-2}$ Pa) [26] were used as was implemented in Booth et al. (2017) [27], Bannan et al. (2019) [28], and Shelley et al. (2020) [14].

The reference compound is placed in a temperature controlled stainless steel Knudsen cell. The cell has an orifice through which the sample effuses creating a molecular beam. The size of the orifice is $\leq 1/10$ the mean free path of the gas molecules in the cell. This ensures that the particles effusing through the orifice do not significantly disturb the thermodynamic equilibrium of the cell [25,29]. The molecular beam is then ionised using a standard 70 eV electron ionisation and analysed using a quadrupole mass spectrometer.

The ionisation cross sections for each compound were estimated by summing the ionisation cross section for each atom in the compound at the ionisation energy (70 eV) [29]. The ionisation cross sections for each atom where taken from the NIST: Electron-impact cross section database [30]. After correcting for the ionisation cross section, the mass spectral signal is proportional to the P^{sat}. Once the calibration process is completed it is possible to measure a sample of unknown P^{sat}. When the sample is changed it is necessary to isolate the sample chamber from the measurement chamber using a gate valve so that the sample chamber can be vented, whilst the ioniser filament and the secondary electron multiplier (SEM) detector can remain on and allow for direct comparisons with the reference compound. The P^{sat} of the sample can be determined from the intensity of the mass spectrum, and the temperature at which the mass spectrum was taken are known. The samples of unknown P^{sat} are typically solid so it is the P_S^{sat} that is determined. After the P_S^{sat} (Pa), has been determined for multiple temperatures, the August equation (Equation (1)) can be used to determine the enthalpy and entropy of sublimation as shown in Booth et al. (2009) [25].

$$\ln\left(P^{\text{sat}}\right) = -\frac{\Delta H_{\text{sub}}}{RT} + \frac{\Delta S_{\text{sub}}}{R} \tag{1}$$

where T is the temperature (K), R is the ideal gas constant (J mol^{-1} K^{-1}), ΔH_{sub} is the enthalpy of sublimation (J mol^{-1}) and ΔS_{sub} is the entropy of sublimation (J mol^{-1} K^{-1}). P^{sat} was obtained over a range of 30 K in this work starting at 298 K and rising to 328 K. The reported solid state vapour pressures are calculated from a linear fit of $\ln(P^{\text{sat}})$ vs. 1/T using the August equation. ΔH_{sub} can be extracted from the gradient of this linear fit and ΔS_{sub} can be extracted from the intercept [4].

2.2. Differential Scanning Calorimetry (DSC)

According to the reference state used in atmospheric models and as predicted by GCMs, P_L^{sat} is required. Therefore, it is necessary to convert the P_S^{sat} determined by the KEMS system into a P_L^{sat}. As with previous KEMS studies [4,14,24] the melting point (T_m) and the enthalpy of fusion (ΔH_{fus}) are required for the conversion. These values were measured with a TA Instruments DSC 2500 Differential Scanning Calorimeter (DSC) sourced from TA Instruments UK, Elstree, UK. Within the DSC, heat flow and temperature were calibrated using an indium reference, and heat capacity using a sapphire reference. A heating rate of 10 K min^{-1} was used, then, 5–10 mg of sample was measured using a microbalance and then pressed into a hermetically sealed aluminium DSC pan. A purge gas of N_2 was used with a flow rate of 30 mL min^{-1}. Data processing was performed using the "Trios" software supplied with the instrument. $\Delta c_{p,\text{sl}}$ was estimated using $\Delta c_{p,\text{sl}} = \Delta S_{\text{fus}}$ [31,32].

2.3. MOPAC2016

MOPAC2016 [33] is a semi empirical quantum chemistry program based on the neglect of diatomic differential overlap (NDDO) approximation [34]. This software was used to calculate the partial charges of the phenolic carbon and the molecular polarisibility (α_m) of the compounds investigated.

3. Theory

3.1. Sub-Cooled Correction

The conversion between P_S^{sat} and P_L^{sat} is done using the Prausnitz equation [35] (Equation (2)).

$$\ln\left(\frac{P_L^{sat}}{P_S^{sat}}\right) = \frac{\Delta H_{fus}}{RT_m}\left(\frac{T_m}{T} - 1\right) - \frac{\Delta c_{p,sl}}{R}\left(\frac{T_m}{T} - 1\right) + \frac{\Delta c_{p,sl}}{R}ln\left(\frac{T_m}{T}\right) \qquad (2)$$

where ΔH_{fus} is the enthalpy of fusion (J mol^{-1}), $\Delta c_{p,sl}$ is the change in heat capacity between the solid and liquid states (J mol^{-1}K^{-1}), T is the temperature (K), and T_m is the melting point (K).

3.2. Vapour Pressure Predictive Techniques

Due to a lack of experimental data for SOA GCMs are often used to predict P^{sat} values. GCMs operate under the principal that the contribution, from a functional group, to a property is constant and that the contribution is unaffected by the base molecule (e.g., the contribution from -OH to a property of interest in ethanol and propanol is the same) [3]. This concept is valid in many instances, however there are many where it is not. The most common of which is when multiple functional groups within a molecule interact with each other, changing each of their relative contributions.

GCMs such as EVAPORATION [9] and SIMPOL [8] predict P^{sat} requiring only chemical structure and target temperature, whereas other GCMs such as the Nannoolal et al. method [6] and the Myrdal and Yalkowsky method [7] also require boiling point (T$_b$), which are known as combined methods. For many of the same reasons as for P^{sat}, there is also a lack of experimental T$_b$ data for SOA and T$_b$ must also be predicted using GCMs. The Nannoolal et al. method [36], the Joback and Reid method [37], and the Stein and Brown method [38] are most commonly used. The Joback and Reid method [37] is not considered in this work because the Stein and Brown method [38] is an improved version and it is known to have many biases [10]. For the combined GCMs the need to also estimate T$_b$ gives rise to another source of error. This size of the error introduced by estimating T$_b$ increases the greater the difference between the estimated T$_b$ and the temperature at which P^{sat} is calculated [11].

Due to many of the GCMs often used to predict P^{sat} of SOA having been originally developed for use with monofunctional compounds and hydrocarbons [25], they do not account for intramolecular interactions or steric effects, which are present in multifunctional compounds. There are also some functionalities that are either poorly represented within the fitting data set of a GCM or not represented at all. If the functionality is poorly represented within a GCM it can lead to overfitting. If the functionality is not represented at all, the effects of the functional group may be misrepresented or ignored entirely. For instance, many GCMs do not account for hydroperoxides (-O-O-H) but do account for both ethers (-O-) and hydroxy (-O-H). If the GCM does not contain a parameter for hydroperoxides it would instead treat the group as a combination of an ether and a hydroxy which would lead to a large error, as chemically these groups are very different [3]. Alternatively, if a GCM contained no parameters for halogens, it would simply ignore any halogen atoms when predicting P^{sat}. GCMs also struggle with the proximity effects and isomers that can occur in multifunctional compounds. The Nannoolal et al. method [6] does contain parameters for -ortho, -meta, -para isomerism, but as soon as a third functional group is added to the aromatic ring it can no longer distinguish between the different isomers.

Despite the previous work to assess the performance of GCMs such as those by Barley and McFiggans (2010) [10] and O'Meara et al. (2014) [11] these assessments were done generally for a wide range of SOA and contained few benzaldehydes in the test set. Barley and McFiggans (2010) [10] only contained 2 benzaldehydes in the test sets and O'Meara et al. (2014) [11] contained no more than 5.

4. Results and Discussion

4.1. Solid State Vapour Pressure

P_s^{sat} measured directly by the KEMS is given in Table 2. Measurements were made at increments of 5 K from 298 K to 328 K for a total of seven measurements (with the exception of compounds that melted during the temperature ramp). A minimum of two KEMS measurements were made for each compound, with each individual measurement calculating P_s^{sat} using both PEG-3 and PEG-4 as reference compounds. P_s^{sat} was then taken as the mean of these four values. In the instances where there were large differences between the calculated P_s^{sat} additional measurements were made. The calculated P_s^{sat} of each KEMS measurement can be found in the accompanying dataset [39]. The August equation (Equation (1)) was used to calculate the enthalpies and entropies of sublimation over the studied temperature range. Overall, the compounds with the highest vapour pressure are incapable of forming hydrogen bonds (H-bonds) as they do not contain any H-bond donors. The compounds that cannot H-bond have on average 50% higher P_s^{sat}, with this discussed in detail in Section 4.2.

Table 2. P_S^{sat} at 298 K, and enthalpies and entropies of sublimation of benzaldehydes determined using KEMS. The compounds below the dashed line are capable of H-bonding in the pure component and those above the dashed line are not.

Compound	P_{298} (Pa)	ΔH_{sub} (kJ mol^{-1})	ΔS_{sub} (J mol^{-1} K^{-1})
Methyl 4-formylbenzoate	3.97×10^{-1}	75.98	247.24
terephthalaldehyde	2.34×10^{-1}	76.66	245.10
2,3,4-trimethoxybenzaldehyde	1.11×10^{-1}	87.51	275.35
2,4-dimethoxy-3-methylbenzaldehyde	1.09×10^{-1}	79.02	246.18
3,4-dimethoxybenzaldehyde	6.64×10^{-2}	91.58	284.67
3-ethoxy-4-methoxybenzaldehyde	5.72×10^{-2}	94.49	293.23
4-dimethylaminobenzaldehyde	5.19×10^{-2}	95.42	295.11
4-diethylaminobenzaldehyde	4.44×10^{-2}	92.28	283.70
2,6-dimethoxybenzaldehyde	7.29×10^{-3}	118.09	355.16
o-vanillin	3.88×10^{-1}	67.75	219.30
3-ethoxy-4-hydroxybenzaldehyde	3.14×10^{-2}	100.35	307.95
Vanillin	2.14×10^{-2}	108.16	330.77
2,5-dihydroxybenzaldehyde	1.63×10^{-2}	102.50	309.66
3-hydroxybenzaldehyde	1.58×10^{-2}	109.90	334.17
4-hydroxybenzaldehyde	5.86×10^{-3}	107.76	318.80
Isovanillin	3.43×10^{-3}	119.00	352.12
2-formylbenzoic acid	1.11×10^{-3}	114.82	328.51

4.2. Sub-Cooled Liquid Vapour Pressure

P_L^{sat} were obtained from the P_S^{sat} using thermochemical data obtained through use of a DSC and Equation (2). The results are detailed in Table 3 for H-bonding compounds and Table 4 for non H-bonding compounds.

Table 3. P_L^{sat} at 298 K, melting point, enthalpy of fusion, entropy of fusion, and the partial charge of the phenolic carbon of the H-bonding benzaldehydes (carboxylic carbon in the case of 2-formyl-benzoic acid).

Compound	P_{298} (Pa)	T_m (K)	ΔH_{fus} (kJ mol^{-1})	ΔS_{fus} (J mol^{-1} K^{-1})	Partial Charge of the Phenolic/Carboxylic Carbon
o-vanillin	6.44×10^{-1}	320.09	19.06	59.55	0.311
3-ethoxy-4-hydroxybenzaldehyde	1.31×10^{-1}	351.70	25.27	71.85	0.244
3-hydroxybenzaldehyde	9.21×10^{-2}	378.98	23.19	61.20	0.272
2,5-dihydroxybenzaldehyde	7.02×10^{-2}	373.15	20.16	54.02	0.329 (intra) 0.184 (inter)
Vanillin	6.73×10^{-2}	356.82	18.88	52.90	0.245
4-hydroxybenzaldehyde	2.78×10^{-2}	391.40	18.60	47.53	0.335
Isovanillin	2.36×10^{-2}	390.34	23.20	59.44	0.167
2-formylbenzoic acid	4.96×10^{-3}	375.12	20.36	54.28	0.621

Table 4. P_L^{sat} at 298 K, melting point, enthalpy of fusion, entropy of fusion and polarisability of the non H-bonding benzaldehydes.

Compound	P_{298} (Pa)	T_m (K)	ΔH_{fus} (kJ mol^{-1})	ΔS_{fus} (J mol^{-1} K^{-1})	α_m (Å^3)
methyl 4-formylbenzoate	1.07×10^{0}	337.21	22.48	66.66	17.424
terephthalaldehyde	9.43×10^{-1}	390.06	16.82	43.11	14.888
2,4-dimethoxy-3-methylbenzaldehyde	2.38×10^{-1}	327.43	22.81	69.66	19.931
2,3,4-trimethoxybenzaldehyde	1.73×10^{-1}	313.63	22.64	72.17	20.658
4-dimethylaminobenzaldehyde	1.57×10^{-1}	349.37	20.24	57.93	18.488
3,4-dimethoxybenzaldehyde	1.38×10^{-1}	321.53	20.77	64.61	18.206
3-ethoxy-4-methoxybenzaldehyde	1.14×10^{-1}	324.96	21.67	66.67	20.071
4-diethylaminobenzaldehyde	6.49×10^{-2}	314.53	18.59	59.11	22.224
2,6-dimethoxybenzaldehyde	4.50×10^{-2}	373.19	25.16	67.43	17.944

When comparing the P_L^{sat} of two compounds direct comparisons were made when only one change occurs between the compounds. If more than one structural change occurs, it becomes difficult to determine the exact cause of the change in P_L^{sat} due to the many competing factors, such as steric effects, inter- and intra- molecular bonding, and interactions between neighbouring groups. In previous KEMS studies where direct comparisons have been made between the P^{sat} of similar compounds this was done in the solid state [13,14]. In this work the comparisons will be done for P_L^{sat} rather than P_S^{sat} as P_L^{sat} is more often used in models and is what is predicted by GCMs allowing for easier comparisons to take place.

For the direct comparisons between compounds the key factors are, in order of apparent importance, if the compounds are capable of forming H-bonds, to what extent these H-bonds are intermolecular vs. intramolecular [14], and if no H-bonds are present, the α_m of the compound. Previous studies have found a strong correlation between α_m and P^{sat} for compounds whose primary interactions are dispersive in nature [40–42].

For compounds that are capable of forming H-bonds, the relative positioning of the functional groups is an important factor in determining the potential strength of these H-bonds, and by extension P^{sat}. Through the inductive and resonance effects the positioning of the functional groups can affect the partial charge on the phenolic carbon and the more positive this value the stronger the H-bonds formed, assuming no other effects such as steric hindrance occur. The phenolic carbon of an aromatic compound is shown in Figure 1. This is discussed in more detail in Shelley at el. (2020) [14].

For compounds that are not capable of forming H-bonds there appears to be a relationship between P^{sat} and the polarisability of the compound. This relationship has been investigated in work done by Staikova et al. (2004, 2005) and Liang and Gallagher (1998).

This relationship between P^{sat} and α_m is strongest for non-polar compounds, gets weaker the more polar the compound of interest becomes, and is weakest for compounds capable of forming H-bonds. The strong correlation between α_m and P^{sat} for nonpolar hydrocarbons is consistent with the fact that α_m is related to the dispersion forces, which are the main component of the intermolecular forces for nonpolar compounds [43]. The poorer performance for polar compounds such as ketones can be explained by the permanent dipoles of these compounds reducing the chance of instantaneous dipoles forming, which are the basis of dispersion interactions.
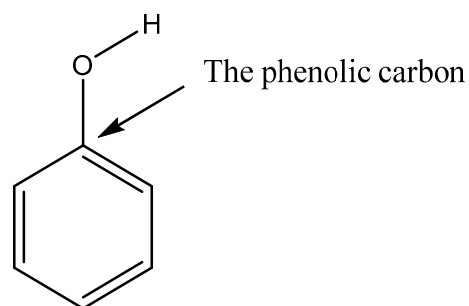
Figure 1. The phenolic carbon on a compound is the carbon directly bonded to the oxygen of the phenol group.

4.2.1. H-Bonding Compounds

Looking first at the compounds capable of H-bonding Figure 2 shows a plot of P_L^{sat} vs. partial charge. In general, as the partial charge of the phenolic carbon increases P_L^{sat} decreases.
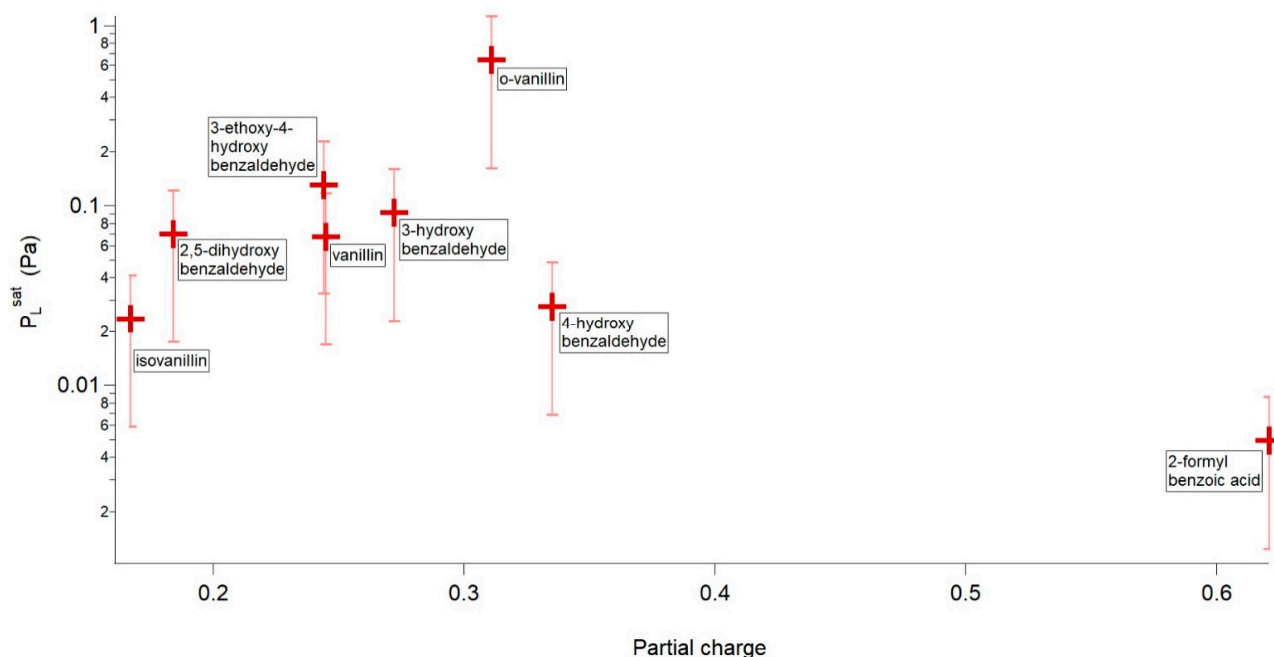
Figure 2. P_L^{sat} vs. partial charge of the phenolic/carboxylic carbon for the compounds capable of H-bonding. Error bars are $\pm75\%$.

Looking at Figure 2 it is obvious that *o*-vanillin is an outlier. *o*-Vanillin has a P_L^{sat} greater than many of the non H-bonding compounds looked at in this study. *o*-Vanillin can be directly compared to its isomers, vanillin and isovanillin, and when looking at the structures of these three compounds the reason for *o*-vanillin's larger P_L^{sat} becomes obvious. Due to the relative positioning of the functional groups around the aromatic ring *o*-vanillin can form an intramolecular H-bond between the H of its phenol group

and O of its aldehyde group, whereas this is not possible for vanillin and isovanillin, as shown in Figure 3. If intramolecular H-bonding dominates, then very little intermolecular H-bonding can occur, leading to an increase in P_L^{sat}. Whilst it is possible for vanillin and isovanillin to form internal H-bonds between the phenol and methoxy groups, it has been shown both theoretically [44] and experimentally [45] that these intramolecular H bonds are weak and the H-bonding is dominated by intermolecular H-bonding.
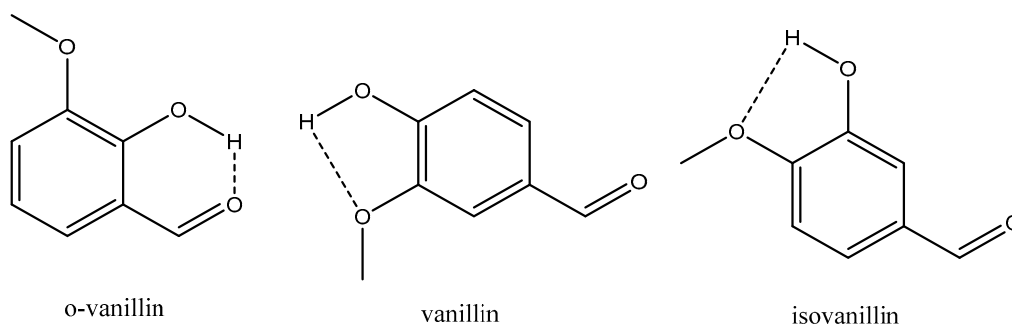
Figure 3. Intramolecular H-bonds of o-vanillin, vanillin and isovanillin. Dashed line illustrates H-bond.

4-hydroxybenzaldehyde can be directly compared to 3-hydroxybenzaldehyde, 3-ethoxy-4-hydroxybenzaldehyde and vanillin, with 4-hydroxybenzaldehyde having a lower P_L^{sat} and larger partial charge of the phenolic carbon than each of these compounds, matching the expected trend as can be seen in Figure 2.

Direct comparisons can also be made between vanillin and 3-ethoxy-4-hydroxybenzaldehyde, with the difference between the two compounds being that the methoxy group of vanillin was replaced with an ethoxy group. Vanillin and 3-ethoxy-4-hydroxybenzaldehyde have almost identical partial charges of their respective phenolic carbons (0.245 vs. 0.244) however the P_L^{sat} of 3-ethoxy-4-hydroxybenzaldehyde is almost double that of vanillin's. This can be explained by the steric hindrance around the phenol group caused by the free rotation of the ethoxy group in 3-ethoxy-4-hydroxybenzaldehyde inhibiting the formation of intermolecular H-bonds leading to a higher P_L^{sat}, shown in Figure 4.
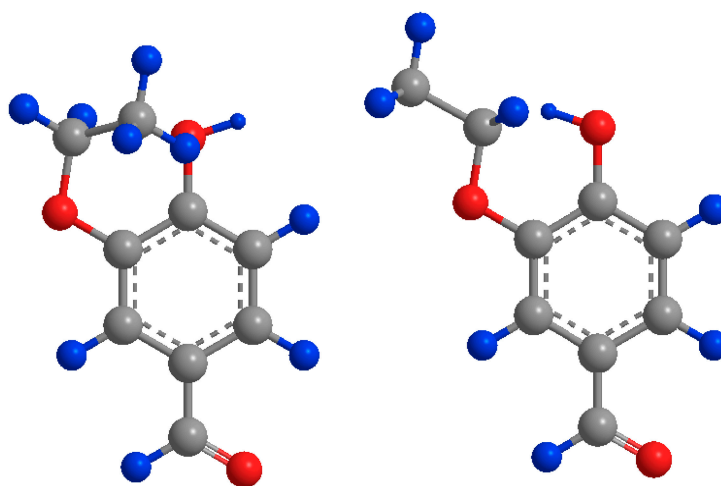
Figure 4. Potential positions of the ethoxy group of 3-ethoxy-4-hydroxybenzaldehyde sterically hindering the oxygen (**left**) and hydrogen (**right**). Carbon atoms (grey) oxygen (red) hydrogen (blue).

2,5-dihydroxybenzaldehyde is a more complex compound to look at as it contains multiple H-bond donors and can form both inter and intramolecular H-bonds. 2,5-dihydroxybenzaldehyde can be compared directly to 3-hydroxybenzaldehyde. Despite 2,5-dihydroxybenzaldehyde being capable of forming two H-bonds compared to

3-hydroxybenzaldehydes one, the P_L^{sat} is not significantly lower as shown in Figure 2. Whilst 2,5-dihydroxybenzaldhyde can form two H-bonds one of these, as shown in Figure 5, is dominated by intra molecular H-bonding. The other hydroxy group has a lower partial charge on the phenolic carbon than 3-hydroxybenzaldehyde. So overall, whilst 2,5-dihydroxybenzaldehyde can form two H bonds, one of these is weaker than the one in 3-hydroxybenzaldehyde and the other is dominated by intramolecular H-bonding.

2,5-dihydroxybenzaldehyde
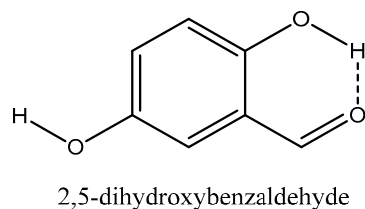
Figure 5. Intramolecular H-bonding of 2,5-dihydroxybenzaldehyde.

Isovanillin can be directly compared to vanillin and 3-hydroxybenzaldehdye and appears to be another outlier. Isovanillin possesses both a lower P_L^{sat} and a lower partial charge of the phenolic carbon than both vanillin and 3-hydroxybenzaldehdye.

4.2.2. Non H-Bonding Compounds

Next, looking at the compounds that are not capable of H-bonding Figure 6 shows a plot of P_L^{sat} vs. α_m. In general, as α_m increases P_L^{sat} decreases.
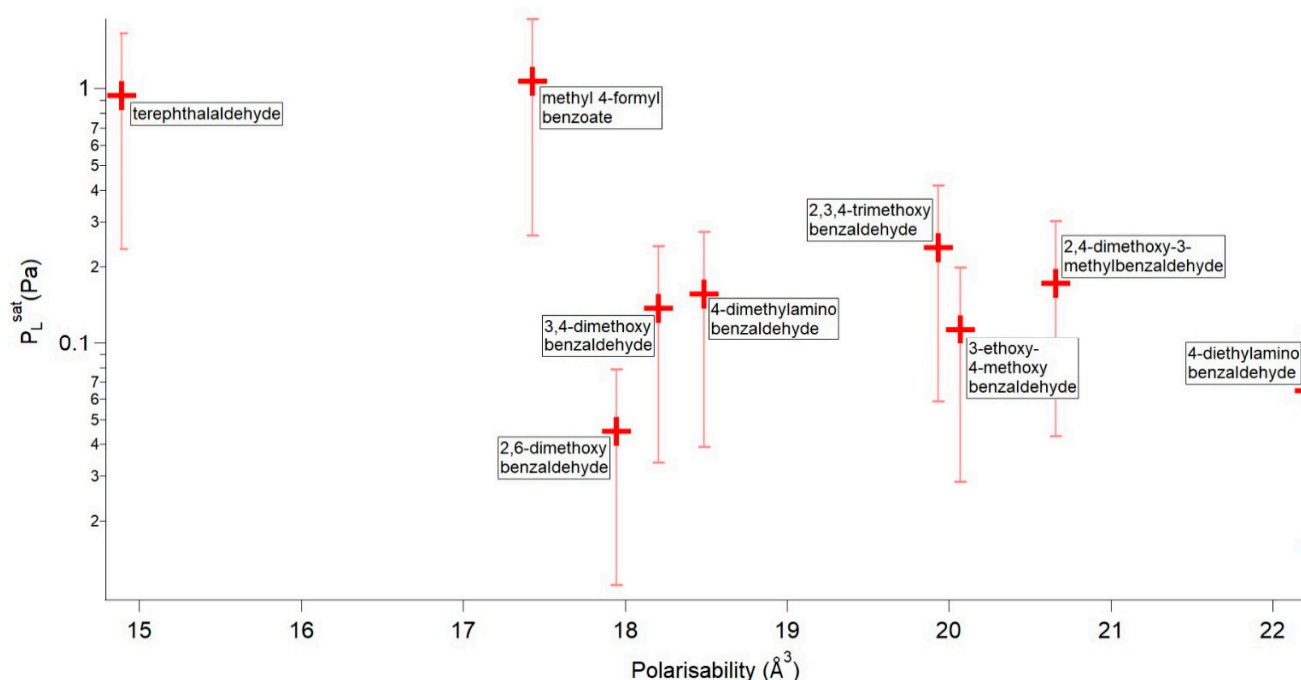
Figure 6. P_L^{sat} vs. α_m for the compounds not capable of forming H-bonds. Error bars are ±75%.

Terephthalaldehyde can be directly compared to 4-dimethylaminobenzaldehyde and 4-diethylaminobenzaldehyde. For these three compounds as α_m increases P_L^{sat} decreases as expected. 2,3,4-trimethoxybenzaldehyde can be directly compared to 2,4-dimethoxy-3-methylbenzaldehyde and 3,4-dimethoxybenzaldehyde. Going from 2,3,4-trimethoxybenzaldehyde to 2,4-dimethoxy-3-methylbenzaldehyde reduces α_m and increases P_L^{sat} as expected. 3,4-dimethoxybenzaldehyde can be directly compared to 3-ethoxy-4-methoxybenzaldehyde and the trend goes as expected with an increase in α_m and a decrease in P_L^{sat}. Methyl 4-formylbenzoate appears to be an outlier with a P_L^{sat} that is

much greater than expected given its α_m. This is difficult to explain and requires further investigation. 2,6-dimethoxybenzaldehyde appears to be another outlier as it has a P_L^{sat} that is lower than would be expected given its α_m.

4.2.3. Comparisons between H-Bonding and non H-Bonding Compounds

Where direct comparisons between the P_L^{sat} of the H-bonding compounds and non H-bonding compounds are possible the P_L^{sat} of the H-bonding compounds are always lower, as would be expected, with the exception of 3-ethoxy-4-hydroxybenzaldehyde and 3-ethoxy-4-methoxybenzaldehyde. The high P_L^{sat} of 3-ethoxy-4-hydroxybenzaldehyde, relative to the other H-bonding compounds in this study, has already been discussed and the same explanation can be applied in this instance where the free rotation of the ethoxy group sterically hindering the formation of H bonds. This leads to the higher P_L^{sat}. Comparing the P_L^{sat} with P_S^{sat} the absolute ordering of the measured P^{sat} changes for some of the compounds. Only two of these changes in order affect the previous discussion. These are 3-ethoxy-4-hydroxybenzaldehyde and 3-ethoxy-4-methoxybenzaldehyde, and 3-hydroxybenzaldehyde and 2,5-dihydroxybenzaldehyde. When accounting the quoted errors P^{sat} ($\pm 75\%$ for sub-cooled liquid and $\pm 40\%$ for solid state [25]) neither of these changes are significant.

4.3. Comparisons with Estimations from GCMs

In Figure 7 the experimentally determined P_L^{sat} of the benzaldehydes are compared to the predicted values of several GCMs. The values used in Figure 7 are included in Table S1. These GCMs are SIMPOL [8], the Nannoolal et al. method [6], and the Myrdal and Yalkowsky method [7]. The Nannoolal et al. method [6] and the Myrdal and Yalkowsky method [7] are both combined methods which require a boiling point to function. For most SOAs the experimental T_b is unknown, therefore a boiling point GCM is required to estimate T_b. In this work the Nannoolal et al. method [36] and the Stein and Brown method [38] are used to estimate T_b. Table 5 shows the mean difference in orders of magnitude between the experimental P_L^{sat} and the predicted P_L^{sat}.
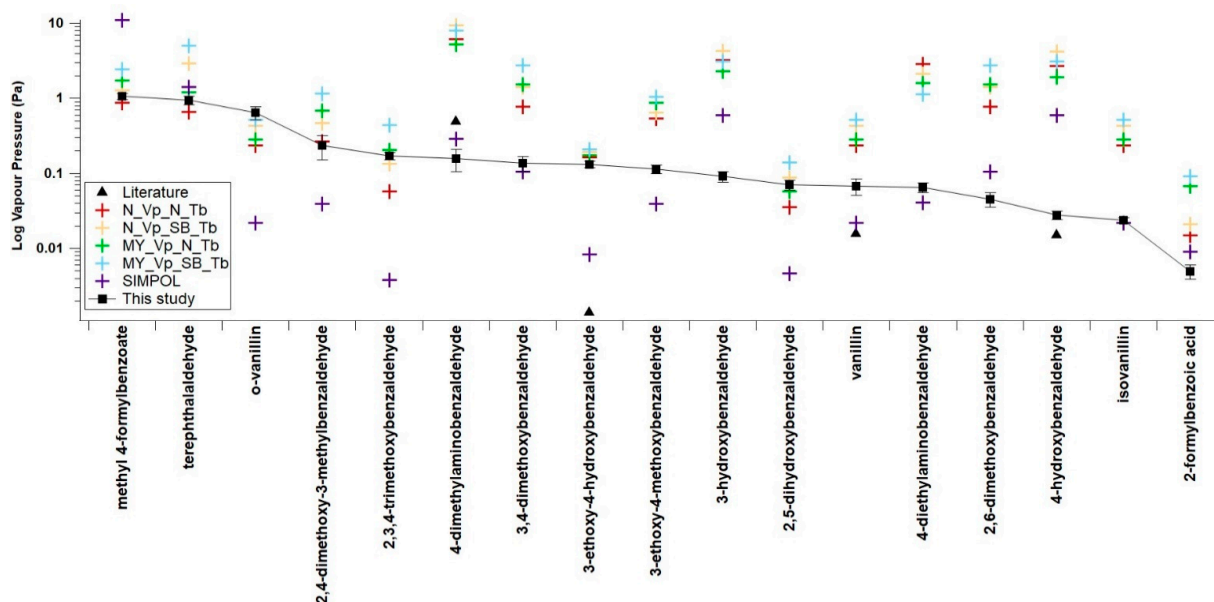
Figure 7. Comparison of estimated and measured sub-cooled saturation vapour pressures. N_Vp (Nanoolal vapour pressure), MY_Vp (Myrdal and Yalkowsky vapour pressure, SIMPOL (SIMPOL vapour pressure), N_Tb (Nannoolal boiling point), SB_Tb (Stein and Brown boiling point), Literature (4-dimethylaminobenzaldehyde from Daubert and Danner [46], 3-ethoxy-4-hydroxybenzaldehyde, vanillin, and 4-hydroxybenzaldehyde from Yaws [47]. Error bars are ± 1 standard deviation.

Table 5. Table showing the average difference between the experimental $P_{\mathrm{L}}^{\mathrm{sat}}$ and the predicted $P_{\mathrm{L}}^{\mathrm{sat}}$. N_VP is the Nannoolal et al. method [6], MY_VP is the Myrdal and Yalkowsky method [7], N_Tb is the Nannoolal et al. method [36], SB_Tb is the Stein and Brown method [38].

	N_VP_N_Tb	N_VP_SB_Tb	MY_VP_N_Tb	MY_VP_SB_Tb	SIMPOL
Average difference (orders of magnitude)	0.60	0.82	0.77	0.98	−0.20

Overall SIMPOL [9] shows the best agreement between the experimental and estimated $P_{\mathrm{L}}^{\mathrm{sat}}$. with a mean difference of −0.20 orders of magnitude with a standard error of 0.203. Eleven of the 17 compounds investigated had estimations within one order of magnitude of the experimental values with the exceptions being methyl 4-formyl benzoate, o-vanillin, 2,3,4-trimethoxybenzaldehyde, 3-ethoxy-4-hydroxybenzaldehyde, 2,5-dihydroxybenzaldehyde and 4-hydroxybenzaldehyde. There appears to be no particular pattern as to which compounds are estimated within one order of magnitude and which are not, as compounds with relatively high, middling, and low $P_{\mathrm{L}}^{\mathrm{sat}}$, as well as both compounds that can, and cannot, be H-bonds are present in this list. All compounds were estimated within two orders of magnitude. SIMPOL [9] has a tendency to underestimate the $P_{\mathrm{L}}^{\mathrm{sat}}$ when applied to the benzaldehydes in this study.

Of the two T_{b} methods used, the Nannoolal et al. method [36] performed better than the Stein and Brown method [38] when used in conjunction with both the Nannoolal et al. method [6] and the Myrdal and Yalkowsky method [7]. This is the reverse of what was observed in the work by Shelley et al. [14] looking at nitroaromatics, including nitrobenzaldehydes, where the Stein and Brown method [38] outperformed the Nanoolal et al. method [36]. This suggests that the Stein and Brown method performs better for compounds containing nitro compounds than the Nannoolal et al. method, but the Nannoolal et al. method is better for benzaldehydes.

The Nannoolal et al. method [6] when used in conjunction with the Nannoolal et al. method [36] has the next best performance when compared to the experimental values in this work. The mean difference is 0.60 orders of magnitude and a standard error of 0.187. 12 of the 17 compounds investigated had estimations within one order of magnitude. The exceptions were 4-dimethylaminobenzaldehyde, 3-hydroxybenzaldehyde, 4-diethylaminobenzaldehyde, 2,6-dimethoxybenzaldehyde and 4-hydroxybenzaldehyde. Unlike with SIMPOL [8] where there appeared to be no apparent pattern, for the Nannoolal et al. method [6] the larger differences between experimental and predicted value occur for the compounds with a lower experimental $P_{\mathrm{L}}^{\mathrm{sat}}$. This is behaviour is common in GCMs as the associated errors of measuring low $P_{\mathrm{L}}^{\mathrm{sat}}$ increases as $P_{\mathrm{L}}^{\mathrm{sat}}$ falls, and differences between different techniques becomes more pronounced. The estimated $P_{\mathrm{L}}^{\mathrm{sat}}$ of all compounds were estimated within 2 orders of magnitude of the experimental values. Whilst the Nannoolal et al. method [6] predicts more of the compounds within one order of magnitude than SIMPOL [8], it still on average, has less accurate predictions. The Nannoolal et al. method [6] has a tendency to overestimate the $P_{\mathrm{L}}^{\mathrm{sat}}$.

The Myrdal and Yalkowsky method [7] when used in conjunction with the Nannoolal et al. method [36] has a mean difference of 0.77 orders of magnitude with a standard error of 0.145. Only 9 of the 17 compounds investigated have $P_{\mathrm{L}}^{\mathrm{sat}}$ within one order of magnitude of the experimental values. Similar to the Nannoolal et al. method. [6] the majority of the compounds that have a difference of more than 1 order of magnitude between the experimental and predicted $P_{\mathrm{L}}^{\mathrm{sat}}$ are the compounds with the lower experimental $P_{\mathrm{L}}^{\mathrm{sat}}$. The estimated $P_{\mathrm{L}}^{\mathrm{sat}}$ of all compounds were estimated within two orders of magnitude of the experimental values.

When separating the compounds in this study into two groups, those that have the potential to act as H-bond donors and those that do not, the performance of the GCMs changes. For the non H-bonding compounds the mean difference reduces for the Nannoolal et al. method [6] and SIMPOL [8] and increases for the Myrdal and Yalkowsky method [7].

For the H-bonding compounds the reverse is true. These differences are not particularly large, as shown in Table 6.

Table 6. Mean order of magnitude difference between the experimental and predicted P_L^{sat}. N_VP is the Nannoolal et al. method [6]. MY_VP is the Mydral and Yalkowsky method [7] N_Tb is the Nannoolal et al. method [36]. SB_Tb is the Stein and Brown method [38].

Compounds	N_VP_N_Tb	N_VP_SB_Tb	MY_VP_N_Tb	MY_VP_SB_Tb	SIMPOL
This study	0.60	0.82	0.77	0.98	−0.20
Non H-bonding—this study	0.58	0.81	0.80	1.02	−0.15
H-Bonding—this study	0.61	0.83	0.72	0.93	−0.24
Nitrobenzaldehyde from Shelley et al. (2020) [14]	3.18	2.50	3.17	2.46	0.29

In Shelley et al. (2020) [14] the order of magnitude differences between the experimental and predicted P_L^{sat} were looked at for a range of nitroaromatic compounds, including nitrobenzaldehydes. With the exception of SIMPOL [8] the other GCMs struggled with predicting P_L^{sat} within 2.5 orders of magnitude. The nitrobenzaldehyde data from Shelley et al. (2020) [14] is compared to the benzaldehyde data from this work in Table 6. SIMPOL has the best agreement with the benzaldehydes in this work and the nitrobenzaldehydes from previous work with both agreeing well within one order of magnitude (−0.20 and 0.29 orders of magnitude respectively). For the Nannoolal et al. method [6] and the Myrdal and Yalkowsky method [7], the differences between the benzaldehydes and the nitrobenzaldehydes are much larger going from under 1 order of magnitude to 2.4 to 3.2 orders of magnitude, depending on the T_b estimation method used. This shows that the Nannoolal et al. method [6] and the Myrdal and Yalkowsky method [7] especially struggle with compounds containing nitro groups, compared to compounds that do not contain a nitro group.

Based on differences between the experimental and predicted P_L^{sat} from the study the authors recommend the use of SIMPOL [8] for benzaldehydes over the other methods investigated. However, users should still be aware that the errors for individual predictions can be much larger than the average and SIMPOL's tendency to underpredict P_L^{sat} for benzaldehydes.

Other previous studies of the P_L^{sat} of multifunctional aromatic compounds such as those by Bannan et al. (2017) [24] and Dang et al. (2019) [13] also showed much larger differences between the experimental P_L^{sat} and the predicted P_L^{sat}. It is now important to understand the sensitivity of modelling studies to the type of uncertainty in P_L^{sat} that are reported in studies of this type.

5. Conclusions

Experimental values for the P_S^{sat} and P_L^{sat} have been obtained using KEMS and DSC for several atmospherically relevant benzaldehydes and other benzaldehydes of similar functionalities.

The differences in P^{sat} have been explained chemically, with the strength of H-bonding being the most important factor where present, and the molecular polarisability being the most important factor when H-bonding is not present. Whilst these are generally the most important factors, they are not the only factors in play. Steric effects caused by the presence of functional groups can also have a major impact as shown by 3-ethoxy-4-hydroxybenzaldehyde. To further investigate the impacts of H-bonding, inductive and resonance effects, and steric effects on P^{sat} more compounds need to be investigated, with select compounds being chosen to probe these effects.

The predictive models consistently predicted the P_L^{sat} to within two orders of magnitude of the experimental P_L^{sat} values. The predictive models predict the P_L^{sat} of benzaldehydes much more accurately than those of other aromatic compounds such as, nitroaromatic compounds [13,14,24] and dihydroxynaphthalenes [24]. The new data presented here

should support studies trying to ascertain the role of benzaldehydes on aerosol growth and human health impacts.

Supplementary Materials: The following are available online at https://www.mdpi.com/2073-4433/12/3/397/s1, Table S1: Estimated sub-cooled liquid vapour pressures at 298 K.

Author Contributions: Conceptualization, P.S., T.J.B., M.R.A., and D.T.; methodology, C.J.P., T.J.B., and P.S.; software, P.S.; formal analysis, P.S. and S.D.W.; investigation, P.S.; resources, C.J.P. and A.G.; data curation, P.S.; writing—original draft preparation, P.S., S.D.W., and C.J.P.; writing—review and editing, P.S, T.J.B., S.D.W., M.R.A., and D.T.; visualization, P.S.; supervision, T.J.B., M.R.A., and D.T.; funding acquisition, D.T. and M.R.A. All authors have read and agreed to the published version of the manuscript.

Funding: The work contained in this paper contains work conducted during a Ph.D. study supported by the Natural Environment Research Council (NERC) EAO Doctoral Training Partnership and is fully-funded by NERC whose support is gratefully acknowledged. Grant ref no is NE/L002469/1. The work by C.J.P. was carried out at the Jet Propulsion Laboratory, California Institute of Technology, under contract with the National Aeronautics and Space Administration (NASA), and was supported by the Upper Atmosphere Research Program and Tropospheric Chemistry Program.

Institutional Review Board Statement: Not applicable.

Informed Consent Statement: Not applicable.

Data Availability Statement: All data in this paper is available from https://doi.org/10.5281/zenodo.4117801 [39].

Conflicts of Interest: The authors declare no conflict of interest.

References

1. Seinfeld, J.H.; Pandis, S.N. *Atmospheric Chemistry and Physics: From Air Pollution to Climate Change*, 3rd ed.; John Wiley & Sons, Incorporated: New York, NY, USA, 2016.
2. Kanakidou, M.; Seinfeld, J.H.; Pandis, S.N.; Barnes, I.; Dentener, F.J.; Facchini, M.C.; van Dingenen, R.; Ervens, B.; Nenes, A.; Nielsen, C.J.; et al. Organic aerosol and global climate modelling: A review. *Atmos. Chem. Phys.* **2005**, *5*, 1053–1123. [CrossRef]
3. Bilde, M.; Barsanti, K.; Booth, M.; Cappa, C.D.; Donahue, N.M.; Emanuelsson, E.U.; McFiggans, G.; Krieger, U.K.; Marcolli, C.; Topping, D.; et al. Saturation Vapor Pressures and Transition Enthalpies of Low-Volatility Organic Molecules of Atmospheric Relevance: From Dicarboxylic Acids to Complex Mixtures. *Chem. Rev.* **2015**, *115*, 4115–4156. [CrossRef] [PubMed]
4. Booth, A.M.; Barley, M.H.; Topping, D.O.; Mcfiggans, G.; Garforth, A.; Percival, C.J. Solid state and sub-cooled liquid vapour pressures of substituted dicarboxylic acids using Knudsen Effusion Mass Spectrometry (KEMS) and Differential Scanning Calorimetry. *Atmos. Chem. Phys.* **2010**, *10*, 4879–4892. [CrossRef]
5. Hallquist, M.; Wenger, J.C.; Baltensperger, U.; Rudich, Y.; Simpson, D.; Claeys, M.; Dommen, J.; Donahue, N.M.; George, C.; Goldstein, A.H.; et al. The formation, properties and impact of secondary organic aerosol: Current and emerging issues. *Atmos. Chem. Phys. Atmos. Chem. Phys.* **2009**, *9*, 5155–5236. [CrossRef]
6. Nannoolal, Y.; Rarey, J.; Ramjugernath, D. Fluid Phase Equilibria Estimation of pure component properties Part 3. Estimation of the vapor pressure of non-electrolyte organic compounds via group contributions and group interactions. *Fluid Phase Equilib.* **2008**, *269*, 117–133. [CrossRef]
7. Myrdal, P.B.; Yalkowsky, S.H. Estimating Pure Component Vapor Pressures of Complex Organic Molecules. *Ind. Eng. Chem. Res.* **1997**, *36*, 2494–2499. [CrossRef]
8. Pankow, J.F.; Asher, W.E. SIMPOL.1: A simple group contribution method for predicting vapor pressures and enthalpies of vaporization of multifunctional organic compounds. *Atmos. Chem. Phys.* **2008**, *8*, 2773–2796. [CrossRef]
9. Compernolle, S.; Ceulemans, K.; Müller, J.F. Evaporation: A new vapour pressure estimation methodfor organic molecules including non-additivity and intramolecular interactions. *Atmos. Chem. Phys.* **2011**, *11*, 9431–9450. [CrossRef]
10. Barley, M.H.; McFiggans, G. The critical assessment of vapour pressure estimation methods for use in modelling the formation of atmospheric organic aerosol. *Atmos. Chem. Phys* **2010**, *10*, 749–767. [CrossRef]
11. O'Meara, S.; Booth, A.M.; Barley, M.H.; Topping, D.; Mcfiggans, G. An assessment of vapour pressure estimation methods. *Phys. Chem. Chem. Phys.* **2014**, *16*, 19453–19469. [CrossRef] [PubMed]
12. Booth, A.M.; Bannan, T.; McGillen, M.R.; Barley, M.H.; Topping, D.O.; McFiggans, G.; Percival, C.J. The role of ortho, meta, para isomerism in measured solid state and derived sub-cooled liquid vapour pressures of substituted benzoic acids. *RSC Adv.* **2012**, *2*, 4430. [CrossRef]

13. Dang, C.; Bannan, T.; Shelley, P.; Priestley, M.; Worrall, S.D.; Waters, J.; Coe, H.; Percival, C.J.; Topping, D. The effect of structure and isomerism on the vapour pressures of organic molecules and its potential atmospheric relevance. *Aerosol. Sci. Technol.* **2019**, *53*, 1–32. [CrossRef]

14. Shelley, P.D.; Bannan, T.J.; Worrall, S.D.; Alfarra, M.R.; Krieger, U.K.; Percival, C.J.; Garforth, A.; Topping, D. Measured solid state and subcooled liquid vapour pressures of nitroaromatics using Knudsen effusion mass spectrometry. *Atmos. Chem. Phys.* **2020**, *20*, 8293–8314. [CrossRef]

15. Caralp, F.; Foucher, V.; Lesclaux, R.; Wallington, T.J.; Michael Hurley, B.D. Atmospheric chemistry of benzaldehyde: UV absorption spectrum and reaction kinetics and mechanisms of the radical C6H5C(O)O2. *Phys. Chem. Chem. Phys.* **1999**, *1*, 3509–3517. [CrossRef]

16. Baghi, R.; Helmig, D.; Guenther, A.; Duhl, T.; Daly, R. Contribution of flowering trees to urban atmospheric biogenic volatile organic compound emissions. *Biogeosciences* **2012**, *9*, 3777–3785. [CrossRef]

17. Thiault, G.; Mellouki, A.; Le Bras, G.; Chakir, A.; Sokolowski-Gomez, N.; Daumont, D. UV-absorption cross sections of benzaldehyde, ortho-, meta-, and para-tolualdehyde. *J. Photochem. Photobiol. A Chem.* **2004**, *162*, 273–281. [CrossRef]

18. Dubtsov, S.N.; Dultseva, G.G.; Dultsev, E.N.; Skubnevskaya, G.I. Investigation of aerosol formation during benzaldehyde photolysis. *J. Phys. Chem. B* **2006**, *110*, 645–649. [CrossRef] [PubMed]

19. Peng, C.-Y.; Yang, H.-H.; Lan, C.-H.; Chien, S.-M. Effects of the biodiesel blend fuel on aldehyde emissions from diesel engine exhaust. *Atmos. Environ.* **2008**, *42*, 906–915. [CrossRef]

20. Magnusson, R.; Nilsson, C.; Andersson, B. Emissions of Aldehydes and Ketones from a Two-Stroke Engine Using Ethanol and Ethanol-Blended Gasoline as Fuel. *Environ. Sci. Technol.* **2002**, *36*, 1656–1664. [CrossRef]

21. Hamilton, J.F.; Webb, P.J.; Lewis, A.C.; Reviejo, M.M. Quantifying small molecules in secondary organic aerosol formed during the photo-oxidation of toluene with hydroxyl radicals. *Atmos. Environ.* **2005**, *39*, 7263–7275. [CrossRef]

22. Jenkin, M.E.; Saunders, S.M.; Wagner, V.; Pilling, M.J. Protocol for the development of the Master Chemical Mechanism, MCM v3 (Part B): Tropospheric degradation of aromatic volatile organic compounds. *Atmos. Chem. Phys.* **2003**, *3*, 181–193. [CrossRef]

23. Bloss, C.; Wagner, V.; Jenkin, M.E.; Volkamer, R.; Bloss, W.J.; Lee, J.D.; Heard, D.E.; Wirtz, K.; Martin-Reviejo, M.; Rea, G.; et al. Development of a Detailed Chemical Mechanism (MCMv3.1) for the Atmospheric Oxidation of Aromatic Hydrocarbons. *Atmos. Chem. Phys.* **2005**, *5*, 641–644. [CrossRef]

24. Bannan, T.J.; Booth, A.M.; Jones, B.T.; O'meara, S.; Barley, M.H.; Riipinen, I.; Percival, C.J.; Topping, D. Measured Saturation Vapor Pressures of Phenolic and Nitro-aromatic Compounds. *Environ. Sci. Technol.* **2017**, *51*, 3922–3928. [CrossRef] [PubMed]

25. Booth, A.M.; Markus, T.; Mcfiggans, G.; Percival, C.J.; Mcgillen, M.R.; Topping, D.O. Design and construction of a simple Knudsen Effusion Mass Spectrometer (KEMS) system for vapour pressure measurements of low volatility organics. *Atmos. Meas. Tech.* **2009**, *2*, 355–361. [CrossRef]

26. Krieger, U.K.; Siegrist, F.; Marcolli, C.; Emanuelsson, E.U.; Gøbel, F.M.; Bilde, M.; Marsh, A.; Reid, J.P.; Huisman, A.J.; Riipinen, I.; et al. A reference data set for validating vapor pressure measurement techniques: Homologous series of polyethylene glycols. *Atmos. Meas. Tech.* **2018**, *11*, 49–63. [CrossRef]

27. Booth, A.M.; Bannan, T.J.; Benyezzar, M.; Bacak, A.; Alfarra, M.R.; Topping, D.; Percival, C.J. Development of lithium attachment mass spectrometry—Knudsen effusion and chemical ionisation mass spectrometry (KEMS, CIMS). *Analyst* **2017**, *142*, 3666–3673. [CrossRef] [PubMed]

28. Bannan, T.J.; Le Breton, M.; Priestley, M.; Worrall, S.D.; Bacak, A.; Marsden, N.A.; Mehra, A.; Hammes, J.; Hallquist, M.; Alfarra, M.R.; et al. A method for extracting calibrated volatility information from the FIGAERO-HR-ToF-CIMS and its experimental application. *Atmos. Meas. Tech.* **2019**, *12*, 1429–1439. [CrossRef]

29. Hilpert, K. Potential of mass spectrometry for the analysis of inorganic high-temperature vapors. In *Proceedings of the Fresenius' Journal of Analytical Chemistry*; Springer: Berlin/Heidelberg, Germany, 2001; Volume 370, pp. 471–478.

30. Atomic Total Energies: Atomic Reference Data for Electronic Structure Calculations. Available online: https://physics.nist.gov/PhysRefData/Ionization/atom_index.html (accessed on 11 March 2021).

31. Mauger, J.W.; Paruta, A.N.; Gerraughty, R.J. Solubilities of Sulfadiazine, Sulfisomidine, and Sulfadimethoxine in Several Normal Alcohols. *J. Pharm. Sci.* **1972**, *61*, 94–97. [CrossRef]

32. Grant, D.J.W.; Mehdizadeh, M.; Chow, A.H.-L.; Fairbrother, J.E. Non-linear van't Hoff solubility-temperature plots and their pharmaceutical interpretation. *Int. J. Pharm.* **1984**, *18*, 25–38. [CrossRef]

33. Stewart, J.J. *MOPAC2016*; Stewart Computational Chemistry: Colorado Springs, CO, USA, 2016.

34. Dewar, M.J.S.; Thiel, W. A semiempirical model for the two-center repulsion integrals in the NDDO approximation. *Theor. Chim. Acta* **1977**, *46*, 89–104. [CrossRef]

35. Prausnitz, J.; Lichtenthaler, R.; de Azevedo, E. *Molecular Thermodynamics of Fluid-Phase Equilibria*; Pearson Education: Upper Saddle River, NJ, USA, 1998.

36. Nannoolal, Y.; Rarey, J.; Ramjugernath, D.; Cordes, W. Estimation of pure component properties Part 1. Estimation of the normal boiling point of non-electrolyte organic compounds via group contributions and group interactions. *Fluid Phase Equilib.* **2004**, *226*, 45–63. [CrossRef]

37. Joback, K.G.; Reid, R.C.; Reid, C. Estimation of pure-component properties from group-contributions. *Chem. Eng. Commun.* **1987**, *157*, 233–243. [CrossRef]

38. Stein, S.E.; Brown, R.L. Estimation of Normal Boiling Points from Group Contributions. *J. Chem. Inf. Comput. Sci.* **1994**, *34*, 581–587. [CrossRef]

39. Shelley, P.D.; Bannan, T.J.; Worrall, S.D.; Alfarra, M.R.; Percival, C.J.; Garforth, A.; Topping, D. *PetrocShelley/Measured_Solid_State_ and_Sub_Cooled_Liquid_Vapour_Pressures_of_Benzaldehydes_Using_KEMS_Data_Set: Pre Release*; Zenodo: Genève, Switzerland, 2020. [CrossRef]

40. Staikova, M.; Wania, F.; Donaldson, D.J. Molecular polarizability as a single-parameter predictor of vapour pressures and octanol–air partitioning coefficients of non-polar compounds: A priori approach and results. *Atmos. Environ.* **2004**, *38*, 213–225. [CrossRef]

41. Staikova, M.; Messih, P.; Lei, Y.D.; Wania, F.; Donaldson, J.D. Prediction of Subcooled Vapor Pressures of Nonpolar Organic Compounds Using a One-Parameter QSPR. *J. Chem. Eng. Data* **2005**, *50*, 438–443. [CrossRef]

42. Liang, C.; Gallagher, D.A. QSPR Prediction of Vapor Pressure from Solely Theoretically-Derived Descriptors. *J. Chem. Inf. Comput. Sci.* **1998**, *38*, 321–324. [CrossRef]

43. Schwarzenbach, R.P.; Gschwend, P.M.; Imboden, D.M. *Environmental Organic Chemistry*; John Wiley & Sons, Incorporated: Hoboken, NJ, USA, 2016; ISBN 9781118767238.

44. Remko, M.; Polcin, J. Theoretical study of the hydrogen bonding ability of phenol and its ortho, meta and para substituted derivatives. *Adv. Mol. Relax. Interact. Process.* **1977**, *11*, 249–254. [CrossRef]

45. Stymne, B.; Stymne, H.; Wettermark, G. Substituent Effects in the Thermodynamics of Hydrogen Bonding as Obtained by Infrared Spectrometry. *J. Am. Chem. Soc.* **1973**, *95*, 3490–3494. [CrossRef]

46. Daubert, T.E.; Danner, R.P. *Physical and Thermodynamic Properties of Pure Chemicals: Data Compilation*; Hemisphere Pub. Corp.: New York, NY, USA, 1989.

47. Yaws, C.L. *Handbook of Vapor Pressure*; Gulf Pub. Co.: Houston, TX, USA, 1994.